

Determination of quadrupole strengths in the $\gamma^*p \rightarrow \Delta(1232)$ transition at $Q^2 = 0.20$ (GeV/c)²

N.F. Sparveris^a, P. Achenbach^b, C. Ayerbe Gayoso^b,
 D. Baumann^b, J. Bernauer^b, A. M. Bernstein^d, R. Böhm^b,
 D. Bosnar^e, T. Botto^d, A. Christopoulou^a, D. Dale^f,
 M. Ding^b, M. O. Distler^b, L. Doria^b, J. Friedrich^b,
 A. Karabarounis^a, M. Makek^e, H. Merkel^b, U. Müller^b,
 I. Nakagawa^c, R. Neuhausen^b, L. Nungesser^b,
 C.N. Papanicolas^{a,*}, A. Piegsa^b, J. Pochodzalla^b, M. Potokar^g,
 M. Seimetz^b, S. Širca^g, S. Stave^d, S. Stiliaris^a, Th. Walcher^b
 and M. Weis^b

^a*Institute of Accelerating Systems and Applications and Department of Physics,
 University of Athens, Athens, Greece*

^b*Institut für Kernphysik, Universität Mainz, Mainz, Germany*

^c*Radiation Laboratory, RIKEN, 2-1 Hirosawa, Wako, Saitama 351-0198, Japan*

^d*Department of Physics, Laboratory for Nuclear Science and Bates Linear
 Accelerator Center, Massachusetts Institute of Technology, Cambridge,
 Massachusetts 02139, USA*

^e*Department of Physics, University of Zagreb, Croatia*

^f*Department of Physics and Astronomy, University of Kentucky, Lexington,
 Kentucky 40206 USA*

^g*Institute Jožef Stefan, University of Ljubljana, Ljubljana, Slovenia*

Abstract

We report new precise $p(\vec{e}, e'p)\pi^0$ measurements at the peak of the $\Delta^+(1232)$ resonance at $Q^2 = 0.20$ (GeV/c)² performed at the Mainz Microtron (MAMI). The new data are sensitive to both the electric quadrupole ($E2$) and the coulomb quadrupole ($C2$) amplitudes of the $\gamma^*N \rightarrow \Delta$ transition. They yield precise quadrupole to dipole amplitude ratios $\text{CMR} = (-5.09 \pm 0.28_{\text{stat+sys}} \pm 0.30_{\text{model}})\%$ and $\text{EMR} = (-1.96 \pm 0.68_{\text{stat+sys}} \pm 0.41_{\text{model}})\%$ for $M_{1+}^{3/2} = (39.57 \pm 0.75_{\text{stat+sys}} \pm 0.40_{\text{model}})(10^{-3}/m_{\pi^+})$. The new results are in disagreement with Constituent Quark Model predictions and in qualitative agreement with models that account for mesonic contributions, including recent Lattice calculations. They thus give further credence to the conjecture of deformation in hadronic systems favoring the attribution of the origin of

deformation to the dominance of mesonic effects.

Key words: EMR, CMR, electro-pion production, nucleon deformation

In recent years an extensive effort has been focused on identifying and understanding the origin of possible non-spherical components in the nucleon wavefunction [1,2,3,4,5,6,7,8,9,10,11,12,13,14,15,16,17,18,19,20,21]. The complex quark-gluon and meson cloud dynamics of hadrons give rise to non-spherical components in their wavefunction which in a classical limit and at large wavelengths will correspond to a "deformation". The most direct evidence of deformation is provided through the measurement of the spectroscopic quadrupole moment which for the proton, the only stable hadron, vanishes identically because of its spin 1/2 nature. Instead the signature of the deformation of the proton is sought in the presence of resonant quadrupole amplitudes ($E_{1+}^{3/2}, S_{1+}^{3/2}$) in the predominantly magnetic dipole ($M_{1+}^{3/2}$) $\gamma^*N \rightarrow \Delta$ transition [22,23]. Non vanishing resonant quadrupole amplitudes will signify that either the proton or the $\Delta^+(1232)$ or more likely both are deformed. The ratios $\text{CMR} = \text{Re}(S_{1+}^{3/2}/M_{1+}^{3/2})$ and $\text{EMR} = \text{Re}(E_{1+}^{3/2}/M_{1+}^{3/2})$ are routinely [17,18,19,20] used to present the relative magnitude of the amplitudes of interest.

Depending on the interpretative framework adopted the origin of the deformation is attributed to a number of different processes. In the constituent-quark picture of hadrons, it arises as a consequence of the non-central color-hyperfine interaction among quarks [1,2], while in dynamical models of the πN system, deformation also arises from the asymmetric coupling of the pion cloud to the quark core. Our current understanding of the nucleon suggests that at long distances (low momenta) the pionic cloud effect dominates while at short distances (high momenta) intra-quark forces predominate. Recent precise experimental results [3,4,5,6,7,8,9,10,11,12,13,14] are in reasonable agreement with predictions of models invoking deformation while at the same time exclude all nucleon models that assume sphericity for the proton and the delta, and thus they confirm the deviation from spherical shape. With the existence of non-spherical components in the nucleon wavefunction well established, recent investigations have focused on understanding the various mechanisms that could generate it.

The measurements reported in this paper have been performed in the low momentum transfer region at $Q^2 = 0.20 \text{ (GeV/c)}^2$ where the pionic contribution is expected to dominate [16,17,18]. The new data taken together with the measurements at the photon point [3,4], at $Q^2 = 0.06 \text{ (GeV/c)}^2$ [24] and

* Corresponding author.

Email address: cnp@iasa.gr (C.N. Papanicolas).

$Q^2 = 0.127 (GeV/c)^2$ [6,13] explore the low Q^2 dependence of the quadrupole amplitudes providing valuable insights into the mechanism that generates the deformation.

The cross section of the $p(\vec{e}, e'p)\pi^0$ reaction is sensitive to five independent partial responses ($\sigma_T, \sigma_L, \sigma_{LT}, \sigma_{TT}$ and $\sigma_{LT'}$) [20] :

$$\frac{d^5\sigma}{d\omega d\Omega_e d\Omega_{pq}^{cm}} = \Gamma(\sigma_T + \epsilon \cdot \sigma_L - v_{LT} \cdot \sigma_{LT} \cdot \cos \phi_{pq}^* + \epsilon \cdot \sigma_{TT} \cdot \cos 2\phi_{pq}^* - h \cdot p_e \cdot v_{LT'} \cdot \sigma_{LT'} \cdot \sin \phi_{pq}^*)$$

where the kinematic factors $v_{LT} = \sqrt{2\epsilon(1+\epsilon)}$ and $v_{LT'} = \sqrt{2\epsilon(1-\epsilon)}$, ϵ is the transverse polarization of the virtual photon, Γ the virtual photon flux, $h = \pm 1$ is the electron helicity, p_e is the magnitude of the longitudinal electron polarization, and ϕ_{pq}^* is the proton azimuthal angle with respect to the electron scattering plane. The virtual photon differential cross sections ($\sigma_T, \sigma_L, \sigma_{LT}, \sigma_{TT}$ and $\sigma_{LT'}$) are all functions of the center of mass energy W , the four momentum transfer squared Q^2 , and the proton center of mass polar angle θ_{pq}^* (measured from the momentum transfer direction) [20].

The $\sigma_0 = \sigma_T + \epsilon \cdot \sigma_L$ response is dominated by the M_{1+} resonant multipole. The interference of the $C2$ and $E2$ amplitudes with the $M1$ dominates the Longitudinal - Transverse (LT) and Transverse - Transverse (TT) responses respectively. The $\sigma_{LT'}$ response [20] provides sensitivity to background contributions [25] primarily through the $Im(S_{0+}^* M_{1+})$ term; as a result the real part of S_{0+} is manifested through interference with the dominant imaginary part of M_{1+} .

The experiment was performed at the Mainz Microtron using the A1 magnetic spectrometers [26] in an arrangement identical to that reported in [14,24]. An 855 MeV polarized electron beam was employed on a liquid-hydrogen target. Beam polarization was measured periodically with a Møller polarimeter to be $\approx 75\%$. The beam average current was 25 μA . Electrons and protons were detected in coincidence with spectrometers A and B respectively. Both spectrometers use two pairs of vertical drift chambers respectively for track reconstruction and two layers of scintillator detectors for timing information and particle identification [26]. Spectrometer B allows out-of-plane detection capability of up to 10° with respect to the horizontal plane which allows access to the fifth response. Measurements with the proton spectrometer at three different azimuthal angles, ϕ_{pq}^* , for the same central kinematics in W, Q^2 and θ_{pq}^* allowed the extraction of all three unpolarized partial cross sections σ_{TT}, σ_{LT} and $\sigma_0 = \sigma_T + \epsilon \cdot \sigma_L$.

Measurements were performed at central kinematics of $W = 1221$ MeV and

$Q^2 = 0.20 (GeV/c)^2$ and at the proton angles of $\theta_{pq}^* = 0^\circ, 33^\circ$ and 57° . At each $\theta_{pq}^* = 33^\circ$ and 57° kinematics, the proton spectrometer was sequentially placed at three different azimuthal angles ϕ_{pq}^* . At the $\theta_{pq}^* = 33^\circ$ setup, the proton spectrometer was placed at $\phi_{pq}^* = 0^\circ, 90^\circ$ and 180° while at $\theta_{pq}^* = 57^\circ$ due to space limitations caused by the beam line it was placed at $\phi_{pq}^* = 38^\circ, 142^\circ$ and 180° . Thus in both cases it became possible to isolate σ_{TT}, σ_{LT} and $\sigma_0 = \sigma_T + \epsilon \cdot \sigma_L$ partial cross sections. The out of plane measurements allowed us to extract the $\sigma_{LT'}$ cross section at both $\theta_{pq}^* = 33^\circ$ and 57° kinematics. In the case of the $\theta_{pq}^* = 33^\circ$ kinematics the extensive phase space coverage of the spectrometers as well as the sufficient statistics allowed the extraction of the partial cross sections at the proton angles of $\theta_{pq}^* = 27^\circ$ and 40° as well.

Systematic uncertainties were reduced by using Spectrometer C throughout the experiment as a luminosity monitor. Elastic scattering data from H and ^{12}C for calibration purposes were taken at 600 MeV. Cross sections were measured at $Q^2 = 0.127 (GeV/c)^2$ [24] at kinematics similar to those of Bates [13]; the two sets of data are statistically compatible insuring that data obtained from the two laboratories can be meaningfully compared as done in Fig. 2.

In Fig. 1 we present the experimental results for $\sigma_o = \sigma_T + \epsilon \cdot \sigma_L, \sigma_{LT}, \sigma_{TT}$ and $\sigma_{LT'}$ compared with the SAID multipole analysis [21], the phenomenological model MAID 2003 [19,18], the dynamical model calculations of Sato-Lee [16] and of DMT (Dubna - Mainz - Taipei) [17] and the ChEFT calculation of Pascalutsa and Vanderhaegen [27]. The SAID multipole analysis [21] describes the data adequately with an overall tendency to overestimate them; it fails to describe the σ_0 measurement at $\theta_{pq}^* = 0^\circ$. The MAID model [18,19] which offers a flexible phenomenology and which was the most successful in describing the $Q^2 = 0.127 (GeV/c)^2$ data [13] overestimates σ_o, σ_{LT} and $\sigma_{LT'}$ thus indicating that a re-adjustment is needed both in the resonant and in the background amplitudes. The Sato-Lee [16] and DMT [17] dynamical models provide a nucleon description which explicitly incorporates the physics of the pionic cloud. Both calculate the resonant channels from dynamical equations. DMT uses the background amplitudes of MAID with some small modifications. Sato-Lee calculate all amplitudes consistently within the same framework with only three free parameters. Both find that a large fraction of the quadrupole multipole strength arises due to the pionic cloud with the effect reaching a maximum value in the region $Q^2 = 0.15 (GeV/c)^2$. Sato-Lee offers a good description of the data slightly overestimating σ_o for proton angles above $\theta_{pq}^* = 50^\circ$. DMT disagrees with the σ_{LT} measurements indicating that the Coulomb quadrupole amplitude is overestimated. The chiral perturbation calculation of Pascalutsa and Vanderhaegen [27] is also presented in Fig. 1. In addition to the predicted central value an estimate of the model uncertainty is provided by calculating the magnitude of the next order terms in the chiral expansion. Clearly the rather large uncertainties that are associated with this calculation render the prediction compatible with the measurements while at the same time making

the need for the next order calculation obvious. It would be very useful if all of the model calculations would also provide similar model errors which will render the comparison of theory and experiment far more meaningful.

The resonant $M_{1+}^{3/2}$, $S_{1+}^{3/2}$ and $E_{1+}^{3/2}$ have been extracted from the measured partial cross sections. A Truncated Multipole Expansion (TME) fit, in which all background contributions are set equal to zero, has been performed fitting all three resonant amplitudes of interest while results have been extrapolated to $W = 1232 \text{ MeV}$. The resulting TME fit is characterized by high χ^2 (see Table 1) demonstrating the inadequacy of this approach due to the neglecting of the important background amplitude contributions. A fit of the three resonant amplitudes has also been performed while taking into account the contributions of background amplitudes from MAID, DMT, SAID and Sato-Lee model predictions; reasonable χ^2 have been obtained. All 3-parameter-fit results are presented in Table 1 in order to exhibit the effect of the model dependence on the extraction of the amplitudes. The adopted values for the extracted multipoles (and their ratios) shown in Table 2, result from the weighted average of the four model fits of Table 1. We adopt the RMS deviation of the fitted central values as indicative of the model uncertainty. The extracted value of $(-5.09 \pm 0.28_{stat+sys})\%$ for the CMR is found to be in good agreement with the value of $(-5.45 \pm 0.42_{stat+sys})\%$ derived from a MAMI asymmetry $p(e, e'p)\pi^0$ measurement [28] where the result is extracted from a MAID re-fit to the data. EMR is precisely determined for the first time at this Q^2 . A precise measurement of the $M_{1+}^{3/2}$ is also provided through this experiment.

Table 2 presents the derived values along with the respective values of the various model predictions; it is evident that for the resonant amplitudes an overall consistency in terms of sign and magnitude among the models considered has emerged. Nevertheless further refinements are needed in order to describe the data accurately and to provide a consistent value for both CMR and EMR. SAID overestimates the data and in particular σ_0 and it underestimates EMR most likely due to the influence of older data in its data base. At this Q^2 the Sato-Lee model provides the best description of the experimentally measured responses; it is no surprise that its values for the CMR and EMR are very close to the experimentally derived ones.

The results reported here, taken together with the results from the photon point and from $Q^2 = 0.06 \text{ (GeV/c)}^2$ [14] and $Q^2 = 0.127 \text{ (GeV/c)}^2$ [13], complete the experimental investigation of the issue of nucleon deformation at low Q^2 . They allow us to draw conclusions on the mechanism behind the deviation from sphericity, in particular on the role of the pion cloud a manifestly low Q^2 mechanism. The derived M_{1+} , EMR and CMR values vary smoothly (see Fig. 2) as expected. The SAID, MAID, DMT and Sato-Lee models are in qualitative agreement with the experimental results; detailed improvements could and should be implemented as commented above and in previous publications.

The results from constituent quark models are known to considerably deviate from the experimental results failing to describe the resonant quadrupole amplitudes and to substantially underestimate the dominant M_{1+} . Two representative calculations are shown in Fig. 2, that of Capstick [2] and of the hypercentral quark model (HQM) [29], which fail to describe the data. It demonstrates that the color hyperfine interaction is inadequate to explain the effect at least at large distances. The recent effective field theoretical (chiral) calculations [27,30], that are solidly based on QCD, also successfully account for the magnitude of the effects giving further credence to the dominance of the meson cloud effect, although as commented above the next order calculation is required.

Finally, recent results from lattice QCD [15] are also of special interest since they are for the first time accurate enough to allow a comparison to experiment. The chirally extrapolated [27] values of CMR and EMR are found to be non zero and negative in the low Q^2 region, in qualitative agreement with the experimental results, thus linking the experimental evidence for deformation directly to QCD. This impressive success highlights the importance of pursuing this avenue with urgency with more precise lattice results using lighter quark masses and further refining the chiral extrapolation procedure.

In conclusion, the data presented here provide a precise determination of both CMR and EMR at $Q^2 = 0.20 (GeV/c)^2$ while the $M_{1+}^{3/2}$ amplitude is simultaneously being determined. The non zero values of the resonant quadrupole amplitudes determined support the conjecture of nucleon deformation. The new data along with those at $Q^2 = 0.127 (GeV/c)^2$ [6,13] and the ones at $Q^2 = 0.06 (GeV/c)^2$ [14] and the photon point provide a clear and consistent picture of the quadrupole amplitudes at low Q^2 ; they nicely match the JLab data at intermediate Q^2 [10]. The quadrupole to dipole amplitude ratios are found to be bigger by an order of magnitude than the values predicted by quark models on account of the noncentral color-hyperfine interaction [2] and consistent in magnitude with the ones predicted from models that take into account the mesonic degrees of freedom [16,17,18,27,30] reinforcing similar conclusions reached at $Q^2 = 0.127 (GeV/c)^2$ and $Q^2 = 0.06 (GeV/c)^2$. Recent chiral effective [27,30] and lattice calculations with a chiral extrapolation to the physical pion mass [15] which provide a direct link to QCD are in agreement with the experimental values.

We would like to thank the MAMI accelerator group and the MAMI polarized beam group for the excellent beam quality combined with a continuous high polarization. We would also like to thank Drs L. Tiator, S. Kamalov, S. Yang, T.-S.H. Lee, M. Vanderhaegen and V. Pascalutsa for their valuable suggestions and calculations. This work is supported at Mainz by the Sonderforschungsbereich 443 of the Deutsche Forschungsgemeinschaft (DFG) and by the program PYTHAGORAS co-funded by the European Social Fund and

National Resources (EPEAEK II).

References

- [1] A. de Rujula, H. Georgi and S.L. Glashow *et al.*, Phys. Rev **D12**, 147 (1975).
- [2] N. Isgur, G. Karl and R. Koniuk, *Phys. Rev.* **D25**, 2394 (1982); S. Capstick and G. Karl, *Phys. Rev.* **D41**, 2767 (1990).
- [3] G. Blanpied *et al.*, Phys. Rev. Lett. **79**, 4337 (1997).
- [4] R. Beck *et al.*, Phys. Rev. Lett. **78**, 606 (1997);
ibid. 79, 4515 (1997) (Erratum).
R. Beck *et al.*, Phys. Rev. **C61**, 35204 (2000).
- [5] V.V. Frolov *et al.*, Phys. Rev. Lett. **82**, 45 (1999).
- [6] T. Pospischil *et al.*, Phys. Rev. Lett. **86**, 2959 (2001).
- [7] C. Mertz *et al.*, Phys. Rev. Lett. **86**, 2963 (2001).
- [8] P. Bartsch *et al.*, Phys. Rev. Lett. **88**, 142001 (2002).
- [9] L.D. van Buuren *et al.*, Phys. Rev. Lett. **89**, 12001 (2002).
- [10] K. Joo *et al.* Phys., Rev. Lett. **88**, 122001 (2002).
- [11] N.F. Sparveris *et al.*, Phys. Rev. **C67**, 058201 (2003).
- [12] C. Kunz *et al.*, Phys. Lett. **B 564**, 21 (2003).
- [13] N.F. Sparveris *et al.*, Phys. Rev. Lett. **94**, 022003 (2005).
- [14] S. Stave *et al.*, nucl-ex/0604013.
- [15] C. Alexandrou *et al.*, Phys. Rev **D69** 114506 (2004); Phys. Rev. Lett. **94**, 021601 (2005).
- [16] T. Sato and T.-S.H. Lee, Phys. Rev. **C63**, 055201 (2001).
- [17] S.S. Kamalov and S. Yang, Phys. Rev. Lett. **83**, 4494 (1999)
- [18] S.S. Kamalov *et al.*, Phys. Lett. **B 522**, 27 (2001).
- [19] D. Drechsel *et al.*, Nucl. Phys. **A 645**, 145 (1999).
- [20] D. Drechsel and L. Tiator, J. Phys. **G18**, 449 (1992)
- [21] R.A. Arndt, *et al.* Phys. Rev. **C66**, 055213 (2002); nucl-th/0301068 and <http://gwdac.phys.gwu.edu>
- [22] C.N. Papanicolas, Eur. Phys. J. **A 18**, 141 (2003).

- [23] A.M. Bernstein, Eur. Phys. J. **A 17**, 349 (2003).
- [24] S. Stave, Ph.D. thesis, MIT, 2006 (to be published).
- [25] W. Mandeville *et al.*, Phys. Rev. Lett. **72**, 3325-3328 (1994).
- [26] K.I. Blomqvist *et al.*, Nucl. Instrum. Methods **A 403**, 263 (1998).
- [27] V. Pascalutsa and M. Vanderhaegen *et al.*, Phys. Rev. Lett. **95**, 232001 (2005)
and V. Pascalutsa and M. Vanderhaegen *et al.*, Phys. Rev. **D73**, 034003 (2006).
- [28] D. Elsner *et al.*, Eur. Phys. J. **A 27** 91-97 (2006).
- [29] M. De Sanctis *et al.*, Nucl. Phys. **A 755**, 294 (2005).
- [30] T. A. Gail and T. R. Hemmert, Eur. Phys. J. **A 28** (1), 91-105 (2006).

Table 1

Values of CMR, EMR and $M_{1+}^{3/2}$ at $W = 1232 \text{ MeV}$ and $Q^2 = 0.20 (\text{GeV}/c)^2$ extracted from the experimental data performing I) a Truncated Multipole Expansion (TME) fit to the data and II) a 3-parameter-fit (resonant amplitudes only) using the background contributions from the MAID, DMT, SAID and Sato-Lee model predictions respectively.

	CMR (%)	EMR (%)	$M_{1+}^{3/2} (10^{-3}/m_{\pi^+})$	$(\chi^2/d.o.f.)$
TME	-5.62 ± 0.26	-3.00 ± 0.67	39.51 ± 0.75	4.75
$fit_{(MAID)}$	-5.50 ± 0.29	-2.36 ± 0.69	39.43 ± 0.75	1.31
$fit_{(DMT)}$	-5.04 ± 0.27	-1.75 ± 0.67	39.84 ± 0.75	0.82
$fit_{(SAID)}$	-4.68 ± 0.28	-1.41 ± 0.67	38.89 ± 0.76	1.52
$fit_{(SL)}$	-5.11 ± 0.27	-2.24 ± 0.69	39.76 ± 0.75	0.89

Table 2

The experimentally derived values of CMR, EMR and $M_{1+}^{3/2}$ at $W = 1232 \text{ MeV}$ and $Q^2 = 0.20 (\text{GeV}/c)^2$ are presented (as extracted from the average of the 3-parameter-fits to the data (listed in Table 1) which include the background amplitude contributions from the MAID, DMT, SAID and SL models). The first errors correspond to the experimental statistical+systematic fitting uncertainties while the second one corresponds to the model uncertainties. The initial model values for the MAID, DMT, SAID, Sato-Lee, Pascalutsa-Vanderhaeghen ChEFT and the Gail-Hemmert predictions for the amplitudes of interest are also presented in the table for comparison.

	CMR (%)	EMR (%)	$M_{1+}^{3/2} (10^{-3}/m_{\pi^+})$
<i>experiment</i>	$-5.09 \pm 0.28 \pm 0.30$	$-1.96 \pm 0.68 \pm 0.41$	$39.57 \pm 0.75 \pm 0.40$
MAID	-6.50	-2.06	39.98
DMT	-6.68	-2.88	39.85
SAID	-5.01	-0.60	39.45
Sato-Lee	-4.58	-3.11	40.48
ChEFT:PV	-9.19 ± 3.00	-3.05 ± 1.20	38.22 ± 5.10
GH	-6.50	-1.60	

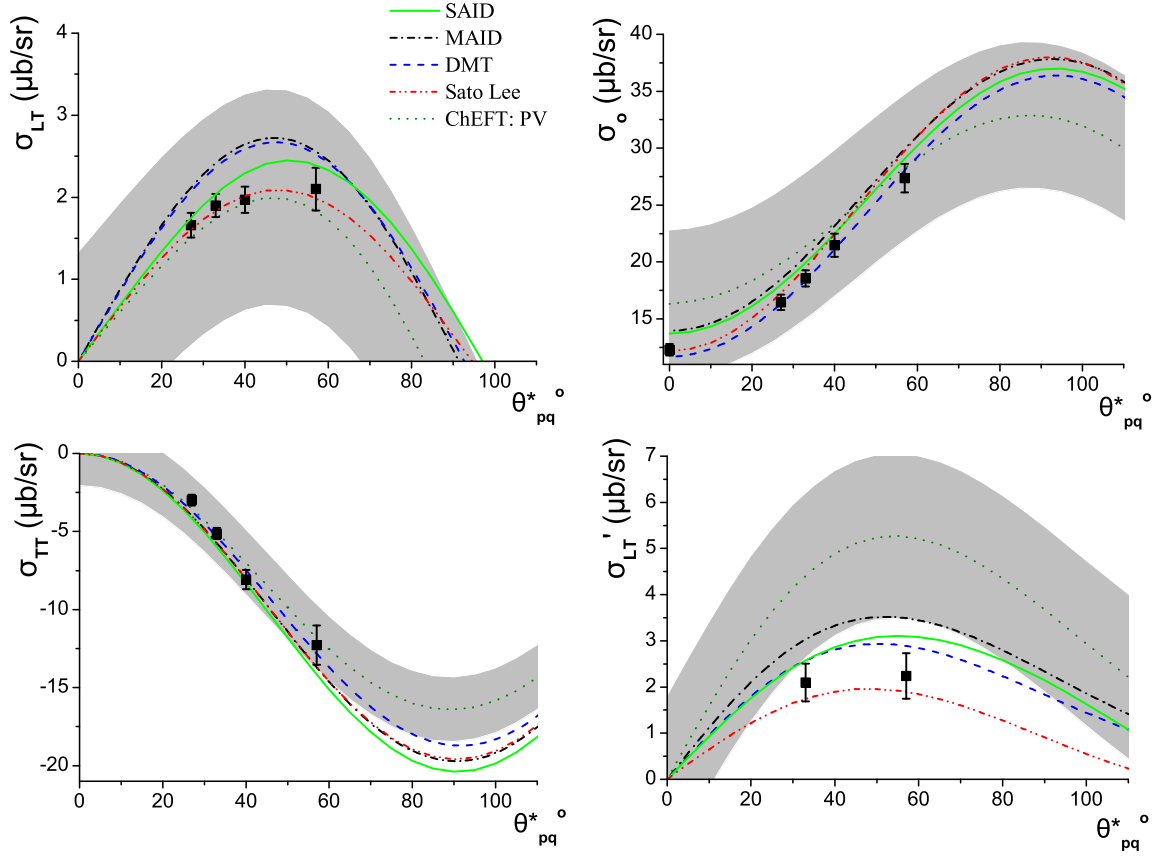


Fig. 1. The measured $\sigma_0 = \sigma_T + \epsilon \cdot \sigma_L$, σ_{LT} , σ_{TT} and $\sigma_{LT'}$ partial cross sections as a function of θ_{pq}^* at central kinematics of $W = 1221 \text{ MeV}$ and $Q^2 = 0.20 (\text{GeV}/c)^2$. The theoretical predictions of MAID, DMT, SAID, Sato-Lee and the ChEFT of Pascalutsa and Vanderhaegen (with the corresponding error band) are also presented.

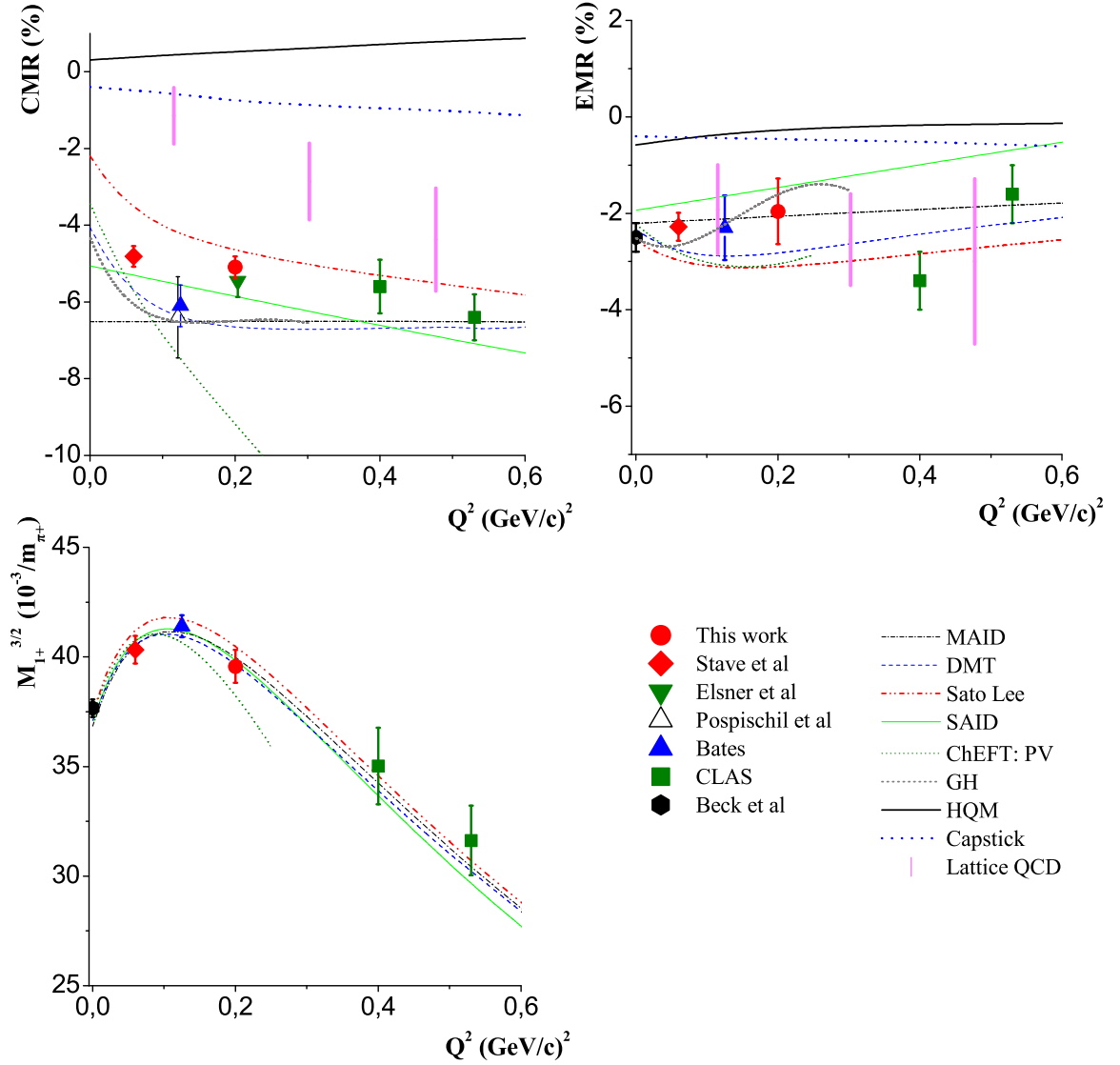


Fig. 2. The extracted values for CMR, EMR and $M_{1+}^{3/2}$ (errors include statistical and systematic uncertainties) as a function of Q^2 . The theoretical predictions of MAID, DMT, SAID, Sato-Lee, ChEFT of Pascalutsa-Vanderhaegen and the Gail-Hemmert and the experimental results from [4,6,10,13,14,28] are shown.